

# Density-matrix functional study of the Hubbard model on one- and two-dimensional bipartite lattices

Matthieu Saubanère and G. M. Pastor

*Institut für Theoretische Physik, Universität Kassel, Heinrich Plett Straße 40, D-34132 Kassel, Germany*

(Received 22 February 2011; revised manuscript received 5 May 2011; published 20 July 2011)

The inhomogeneous Hubbard model is investigated in one and two dimensions by using lattice density-functional theory (LDFT). The ground-state energy  $E = T + W$  is regarded as a functional of the single-particle density matrix  $\gamma$ , where  $T[\gamma]$  represents the kinetic and crystal-field energy, and  $W[\gamma]$  the interaction energy. Besides the known functional  $T[\gamma]$  we propose a simple scaling approximation to the interaction energy  $W[\gamma]$ , which is based on exact results for the Hubbard dimer and on a scaling hypothesis within the domain of representability of  $\gamma$ . As applications we consider the Hubbard model on one- and two-dimensional bipartite lattices. Several ground-state properties are determined including the kinetic and Coulomb energy, density distribution, nearest-neighbor bond order, and charge gap. Comparison with exact Lanczos diagonalizations shows that LDFT with the scaled dimer approximation to  $W[\gamma]$  yields a quite accurate description of the interplay between correlations and charge redistributions, from weak to strong coupling regimes, and for all band fillings. Goals and limitations of the present approach are discussed.

DOI: [10.1103/PhysRevB.84.035111](https://doi.org/10.1103/PhysRevB.84.035111)

PACS number(s): 71.15.Mb, 71.10.Fd, 71.45.Lr, 71.27.+a

## I. INTRODUCTION

In the course of the past few decades, density-functional theory (DFT) has become one of the most successful approaches to study the physics of the many-body problem. The main revolutionary concept behind DFT, as discovered by Hohenberg and Kohn, is to consider the electronic density distribution  $\rho(\vec{r})$  instead of the wave function as the fundamental variable of the many-body problem.<sup>1</sup> In particular the energy  $E$  of any electronic system is expressed as a functional of  $\rho(\vec{r})$  by splitting it into two main groups of terms. The first one depends explicitly on the system under study through the external potential  $V_{\text{ext}}(\vec{r})$  acting on the electrons. This typically involves the ion-electron potential and any other external fields. The second type of contribution describes intrinsic properties of the electronic system, namely, the kinetic energy  $T[\rho]$  and the interaction energy  $W[\rho]$ . These are universal functionals of  $\rho(\vec{r})$  in the sense that they are independent of the considered external potential describing a specific system. The ground-state properties can then be found by implementing a variational procedure with respect to  $\rho(\vec{r})$ , for example, as in the Kohn-Sham scheme.<sup>2</sup> The DFT formulation enjoys general validity and has been successfully applied to an incredibly large variety of physical problems, well-beyond the initial scope of the inhomogeneous electron gas.<sup>3,4</sup>

Recently, several investigations have been performed by applying the concepts of DFT to strongly correlated electrons on a lattice, which are described by means of many-body models such as the Anderson model, the Hubbard model, and related Hamiltonians.<sup>5-7</sup> The study of lattice Hamiltonians in the framework of DFT defines an interesting open problem which seems particularly challenging from various perspectives. On the one side, understanding the physics of strongly correlated electronic systems constitutes a very important theoretical issue. Only very few exact analytical results are available<sup>8-12</sup> and accurate numerical calculations are very demanding.<sup>13-15</sup> Taking into account the general

validity of the concepts of DFT and the remarkable success of its applications to conventional materials, it is reasonable to expect that DFT should provide a new valuable insight into the physics of strong correlations. This presupposes that sound approximations to the interaction- and kinetic-energy functionals are obtained, which remain reliable at all interaction regimes. On the other side, from the perspective of DFT in the continuum, it is well known that the usual local-density and generalized-gradient approximations to the exchange and correlation energy-functional<sup>2-4,16</sup> fail systematically to describe strong interactions in narrow bands. This is the case, for example, in problems involving a separation of charge and spin degrees of freedom or showing correlation-induced localization.<sup>15,17</sup> Therefore, it is also important to understand the reasons behind these drawbacks in order to improve the applicability of DFT to more complex strongly interacting systems. The information inferred from DFT studies of lattice Hamiltonians could thus provide new insights into the properties of the universal kinetic- and interaction-energy functionals.

Among the previous DFT investigations of lattice models one should mention the determination of band gaps in semiconductors,<sup>18</sup> the study of the role of off-diagonal elements of the density matrix and the noninteracting  $v$  representability in a strongly correlated system,<sup>19</sup> and the development of energy functionals of the density matrix with applications to the Hubbard and Anderson models.<sup>20</sup> More recently, an exchange and correlation energy-functional of the site occupations has been derived on the basis of the Bethe-ansatz solution of the one-dimensional Hubbard model.<sup>21</sup> Time-dependent effects have also been investigated.<sup>22</sup> An alternative to these approaches is provided by lattice density-functional theory (LDFT) which considers the single-particle density matrix  $\gamma$  as the basic variable.<sup>23-26</sup> An extension of the Hohenberg-Kohn theorem has been derived by using Levy's correlation-energy functional.<sup>27</sup> In this way the ground-state energy is expressed as the functional  $E[\gamma]$  of the density matrix.<sup>23</sup> Moreover, a variational scheme allows one

to determine the ground-state energy  $E_{\text{gs}}$  and  $\gamma_{\text{gs}}$  from the minimization of  $E[\gamma]$ . In contrast to Hohenberg-Kohn-Sham's DFT, which approximates both the kinetic and Coulomb energy through the so-called exchange and correlation functional  $E_{\text{xc}}[\rho(\vec{r})]$ , a simple exact expression for the kinetic energy  $T[\gamma]$  of the electrons in the lattice is available in LDFT. However, a closed expression for the Coulomb-energy functional  $W[\gamma]$  remains unknown. In Ref. 24 an approximation to  $W$  has been derived for the homogeneous Hubbard model by using exact dimer results and by taking advantage of the scaling properties of  $W[\gamma]$ . Although the accuracy of the applications to a variety of systems has been very encouraging,<sup>24–26</sup> the previous functionals can only be used in periodic lattices showing a uniform density distribution (i.e.,  $\gamma_{ii} = \langle \hat{n}_i \rangle = N_e/N_a$  for all  $i$ ). This is a serious limitation, since charge transfers and inhomogeneities are known to play an important role in many physical problems such as high- $T_C$  superconductivity, alloys, magnetic impurities in metals, etc.<sup>28–30</sup> In fact, it is the ability to cope with inhomogeneous density distribution that gives the true measure of the quality of a DFT approach.<sup>1</sup>

In order to investigate this problem we have recently calculated the interaction energy  $W[\gamma]$  of the Hubbard model on a variety of inhomogeneous one-dimensional (1D) and two-dimensional (2D) lattices as a function of the orbital occupation  $\gamma_{ii}$  and nearest-neighbor bond order  $\gamma_{ij}$ .<sup>31</sup> This study shows that the functional dependence of  $W[\gamma]$  is nearly independent of the system size and band filling provided that  $W$  is scaled between its weakly and strongly correlated limits and that  $\gamma_{ij}$  is scaled within the domain of representability of the density matrix.<sup>31</sup> It is the purpose of this paper to exploit the scaling properties of  $W[\gamma]$  in order to derive a simple explicit approximation to  $W$  in the Hubbard model. As applications of the theory, several representative examples of 1D and 2D bipartite lattices are considered by varying systematically the strength of the crystal fields and Coulomb interactions.

The remainder of the paper is organized as follows. In Sec. II we present the theoretical background about the model and the formulation of LDFT. Section III introduces an explicit approximation to the interaction energy  $W[\gamma]$  as a function of the single-particle density matrix  $\gamma$ , which is suitable for calculations on arbitrary bipartite lattices. This approximation is based on exact analytical results for the Hubbard dimer and a scaling hypothesis on the functional dependence of  $W$  within its domain of representability. In Sec. IV the method is applied to 1D and 2D finite lattices with periodic boundary conditions and the results are discussed. The LDFT calculations are systematically compared with exact Lanczos diagonalizations,<sup>32</sup> in order to assess the accuracy of the approximation to  $W$ . Finally, we close in Sec. V by presenting a summary of conclusions and some interesting future perspectives.

## II. DENSITY-FUNCTIONAL THEORY ON A LATTICE

To be explicit we focus on the inhomogeneous Hubbard model on bipartite lattices, which is expected to capture the main interplay between electron delocalization, correlations,

and charge-density redistributions in narrow-band systems. The Hamiltonian is given by

$$\hat{H} = \sum_{i,\sigma} \varepsilon_i \hat{n}_{i\sigma} + \sum_{(i,j)\sigma} t_{ij} \hat{c}_{i\sigma}^\dagger \hat{c}_{j\sigma} + U \sum_i \hat{n}_{i\downarrow} \hat{n}_{i\uparrow}, \quad (1)$$

where  $\varepsilon_i$  denotes the site-dependent energy levels,  $t_{ij}$  the nearest-neighbor (NN) hopping integrals, and  $U$  the on-site interaction.<sup>7</sup> As usual,  $\hat{c}_{i\sigma}^\dagger$  ( $\hat{c}_{i\sigma}$ ) stands for the creation (annihilation) operator for an electron with spin  $\sigma$  at site  $i$  ( $\hat{n}_{i\sigma} = \hat{c}_{i\sigma}^\dagger \hat{c}_{i\sigma}$ ). The hopping elements  $t_{ij}$  define the dimensionality and structure of the lattice as well as the range of the single-particle hybridizations. The energy levels  $\varepsilon_i$  describe the arrangement of different elements in the lattice or the effect of external fields.<sup>33</sup> The model parameters  $\varepsilon_i$  and  $t_{ij}$  specify the system under study and thus play the role given in conventional DFT to the external potential  $v_{\text{ext}}(\vec{r})$ . Consequently, the basic variable in a density-functional theory of lattice models is the single-particle density matrix  $\gamma_{ij}$  with respect to the sites  $i$  and  $j$ . This involves not only the diagonal elements  $\gamma_{ii}$ , which describe the charge distribution, but also the off-diagonal elements or bond orders  $\gamma_{ij}$ , which give a measure of the degree of electron delocalization. Notice that the dependence on the off-diagonal elements of  $\gamma_{ij}$  results from the nonlocality of the hopping integrals. A similar situation appears in the continuum, if one considers nonlocal pseudopotential.<sup>34</sup>

The ground-state energy  $E_{\text{gs}}$  and density matrix  $\gamma_{ij}^{\text{gs}}$  are determined by minimizing the energy functional

$$E[\gamma] = T[\gamma] + W[\gamma] \quad (2)$$

with respect to  $\gamma_{ij}$ .  $E[\gamma]$  is defined for all density matrices that derive from a physical state, i.e., that can be written as

$$\gamma_{ij} = \sum_{\sigma} \gamma_{ij\sigma} = \sum_{\sigma} \langle \Psi | \hat{c}_{i\sigma}^\dagger \hat{c}_{j\sigma} | \Psi \rangle, \quad (3)$$

where  $|\Psi\rangle$  is an  $N$ -particle state. A density matrix  $\gamma$  is said to be pure-state  $N$  representable if and only if there is an  $N$ -particle state  $|\Psi\rangle$  from which  $\gamma_{ij}$  is derived according to Eq. (3).<sup>35</sup> In this context it is also useful to distinguish the pure-state interacting  $v$ -representable  $\gamma_{ij}$ , or simply  $v$ -representable  $\gamma_{ij}$ , which are defined as the density matrices that can be derived from a ground state of Eq. (1). In other words, a  $v$ -representable  $\gamma_{ij}$  is equal to  $\gamma_{ij}^{\text{gs}}$  for some values of  $\varepsilon_i$ ,  $t_{ij}$ , and  $U$ .

The single-particle contributions to the energy are given by

$$T[\gamma] = \sum_i \varepsilon_i \gamma_{ii} + \sum_{i \neq j} t_{ij} \gamma_{ij}. \quad (4)$$

The first term in Eq. (4) is the charge-density (CD) energy  $E_{\text{CD}}[\gamma_{ii}]$ , which depends only on the diagonal elements of  $\gamma$ . The second one is the kinetic energy  $E_{\text{K}}[\gamma_{ij}]$  associated with the delocalization of the electrons in the lattice. It depends on the off-diagonal elements of  $\gamma$  for which  $t_{ij} \neq 0$ , typically for nearest-neighbor  $ij$ . Notice that the present formulation involves no approximation of the functional dependencies of  $E_{\text{CD}}$  and  $E_{\text{K}}$ . Consequently, all changes in the single-particle energy  $T$  resulting from electronic correlations are taken into account exactly.

The second term in Eq. (2) is the interaction-energy functional. It can be written in terms of the constrained search minimization<sup>27</sup>

$$W[\gamma] = \min_{\Psi \rightarrow \gamma} \left[ U \sum_i \langle \Psi[\gamma] | \hat{n}_{i\uparrow} \hat{n}_{i\downarrow} | \Psi[\gamma] \rangle \right] \quad (5)$$

running over all  $N$ -particle states  $|\Psi[\gamma]\rangle$  that satisfy

$$\langle \Psi[\gamma] | \sum_{\sigma} \hat{c}_{i\sigma}^{\dagger} \hat{c}_{j\sigma} | \Psi[\gamma] \rangle = \gamma_{ij} \quad (6)$$

for all  $i$  and  $j$ . It is important to notice that Eq. (6) defines the set of  $N$ -particle states  $|\Psi\rangle$  within which the minimization is performed. The  $N$  representability of  $\gamma$  ensures that this set is not empty [see Eq. (3)]. It is this constraint on  $|\Psi\rangle$ , which depends of course on  $\gamma$ , that establishes the fundamental functional dependence of the interaction energy  $W$  on the single-particle density matrix. Conceptually, this equation is different from Eq. (3), which expresses the  $N$ -representability condition on  $\gamma$ . In the present formulation  $W[\gamma]$  is only defined for the physically relevant  $N$ -representable  $\gamma$ , since otherwise the minimization set implied in Eq. (5) would be empty.

For repulsive interactions  $W[\gamma]$  represents the minimum value of the average number of double occupations that is compatible with a given density matrix  $\gamma$ , i.e., that corresponds to a given charge distribution and degree of electron delocalization.  $W$  is a universal functional of  $\gamma$  in the sense that it is independent of the system under study, the latter being defined by the external parameters  $\varepsilon_i$  and  $t_{ij}$ . However,  $W$  depends on the number of electrons  $N_e = \sum_i \gamma_{ii}$ , on the internal structure of the many-body Hilbert space, as defined by  $N_e$  and the number of atoms or sites  $N_a$ , and on the model used for the many-body interactions, in the present case Hubbard's on-site form. It is often convenient to express  $W$  in terms of the Hartree-Fock energy  $E_{\text{HF}}$  and the correlation energy  $E_C$  as  $W = E_{\text{HF}} + E_C$ . Here we assume that  $E_{\text{HF}}$  includes the exchange energy, so that  $E_C$  represents only the contribution of correlations.

In this context it is interesting to analyze the dependence of  $W[\gamma]$  on the interaction parameter  $U$ , since this reveals rigorous constraints to be satisfied by any explicit approximation. Once the sign of  $U$  is defined, it is clear that the minimization in Eq. (5) and the representability constraints given by Eq. (6) are independent of  $U$ . Therefore, we may write

$$W[\gamma] = U \min_{\Psi \rightarrow \gamma} \left[ \sum_i \langle \Psi[\gamma] | \hat{n}_{i\uparrow} \hat{n}_{i\downarrow} | \Psi[\gamma] \rangle \right] \quad (7)$$

for all  $U > 0$ , from which the strict linearity of  $W[\gamma]$  as a function of  $U$  follows. This important property is a consequence of the fact that the density matrix  $\gamma$  univocally defines all single-particle contributions. The situation is different in the DFT of the continuum, since the electronic density  $n(\vec{r})$  is not enough to define the kinetic energy unambiguously. Therefore, the Hohenberg-Kohn or Levy-Lieb functionals reflect the compromise of minimizing the sum  $T + W$  of the kinetic and Coulomb energies for a given  $n(\vec{r})$ . In the context of lattice models (in particular for the Hubbard model) there have been attempts to describe the many-body problem in the spirit of the continuum DFT, by considering only the orbital occupations  $n_i = \langle \hat{n}_i \rangle = \gamma_{ii}$  as fundamental variables.<sup>18,21</sup> In this case a

nonlinear dependence of the exchange and correlation (XC) energy as a function of  $U/t$  needs to be assumed, since the kinetic energy is implicitly added to the interaction term when constructing the XC functional. Notice that the kinetic energy of electrons in a lattice cannot be defined by the diagonal  $\gamma_{ii}$  alone. For example,  $\gamma_{ii}$  in a homogeneous system is independent of  $i$  and of  $U/t$ . Therefore,  $\gamma_{ii}$  does not allow us to discern between weakly and strongly correlated states. While such occupation-number approaches are formally correct, the resulting functionals are not universal. In contrast to the continuum, the kinetic-energy operators corresponding to different lattices are different. Therefore, the transferability of local functionals does not seem obvious.

Finally, the variational principle for the ground-state density matrix  $\gamma_{ij}^{\text{gs}}$  follows from the relations<sup>27</sup>

$$E_{\text{gs}} \leq E[\gamma] = T[\gamma] + W[\gamma] \quad (8)$$

for all pure-state  $N$ -representable  $\gamma$  and

$$E_{\text{gs}} = T[\gamma^{\text{gs}}] + W[\gamma^{\text{gs}}], \quad (9)$$

where  $E_{\text{gs}} = \langle \Psi_{\text{gs}} | \hat{H} | \Psi_{\text{gs}} \rangle$  stands for to the ground-state energy. The present formulation of LDFT can be generalized to arbitrary forms of the two-body interaction  $V_{ijkl} c_{i,\sigma}^{\dagger} c_{j,\sigma'}^{\dagger} c_{k,\sigma'} c_{l,\sigma}$ , for example, to site-dependent Coulomb repulsion or Anderson impurity models.<sup>25,37</sup>

### III. SCALING APPROXIMATION TO THE INTERACTION-ENERGY FUNCTIONAL

Once the density-functional variational scheme is established, the challenge is to find a good explicit approximation to the interaction-energy functional which correctly describes the interplay between correlation, delocalization, and charge transfers. In a previous paper<sup>31</sup> we have investigated the properties of  $W[\gamma]$  by performing exact numerical diagonalization on 1D bipartite finite rings with periodic boundary conditions. This study revealed that the dependence of  $W$  as a function of the NN bond order  $\gamma_{12}$  can be considered to be approximately independent of the system size, lattice dimension, and band filling  $n$ , provided that two simple scaling conditions are taken into account. First,  $W(\gamma_{12})$  must be scaled between the limit of weak correlation  $W^0 = \sum_i \gamma_{i\uparrow} \gamma_{i\downarrow}$  and the limit of strong correlation  $W^{\infty} = \sum_i \max[\gamma_{ii} - 1, 0]$ , corresponding to the given charge distribution  $\gamma_{ii}$ . Second,  $\gamma_{12}$  must be scaled accordingly in the range  $\gamma_{12}^{\infty} < \gamma_{12} < \gamma_{12}^0$  between the strongly correlated limit  $\gamma_{12}^{\infty}$  and the weakly correlated limit  $\gamma_{12}^0$ . This range represents the domain of  $v$  representability of  $\gamma$ . Mathematically, this means that for a given density distribution  $\{\gamma_{ii}\}$  it is a good approximation to regard

$$w = \frac{W - W^{\infty}}{W^0 - W^{\infty}} \quad (10)$$

as a function of the degree of electron delocalization

$$g_{12} = \frac{\gamma_{12} - \gamma_{12}^{\infty}}{\gamma_{12}^0 - \gamma_{12}^{\infty}}. \quad (11)$$

In other words, the relative change in  $W$  associated with a change in the degree of electron delocalization  $g_{12}$  can be considered as nearly independent of the system under study.

This extends the conclusions of previous investigations on the homogeneous Hubbard model.<sup>23</sup> Notice, however, that the relation between  $w$  and  $g_{12}$  does depend on  $\gamma_{ii}$  and in particular on the charge transfer  $\Delta n = \gamma_{22} - \gamma_{11}$  between the sublattices of a bipartite structure.<sup>38</sup> Consequently, a sound general approximation to  $W$  can be obtained by scaling the functional dependence of  $W$  on  $\gamma_{ij}$  corresponding to a simple reference system, which already contains the fundamental interplay between delocalization, charge transfer, and correlations.

The Hubbard dimer is the smallest and simplest system that fulfills these conditions. We therefore propose the scaled dimer approximation  $W_{\text{sc}}$ , which is given by

$$\frac{W_{\text{sc}} - W^\infty}{W^0 - W^\infty} = \frac{W_2 - W_2^\infty}{W_2^0 - W_2^\infty}, \quad (12)$$

where the subindex 2 refers to the dimer. Using the definition of  $w$  [Eq. (10)] one may write Eq. (12) in a compact form as  $w_{\text{sc}}(g_{12}, \Delta n) = w_2(g_{12}, \Delta n)$ , which implies

$$W_{\text{sc}} = W^\infty + (W^0 - W^\infty) \frac{W_2 - W_2^\infty}{W_2^0 - W_2^\infty}. \quad (13)$$

Notice that all the terms on the right-hand side of Eq. (13) are simple functions of  $\gamma_{ij}$ . The uncorrelated and strongly correlated bounds in the dimer ( $N_e = N_a = 2$ ) are given by  $W_2^0 = [1 + (\Delta n/2)^2]/4$  and  $W_2^\infty = \Delta n/4$ . For an arbitrary system, these bounds are given by  $W^0 = \sum_i \gamma_{ii} \uparrow \gamma_{ii} \downarrow$  (Hartree-Fock limit) and  $W^\infty = \sum_i \max[\gamma_{ii} - 1, 0]$  (minimal double occupations).<sup>39</sup> Finally, the exact dimer interaction-energy functional for  $N_e = 2$  is given by

$$\frac{W_2}{UN_a} = \begin{cases} 1 - \frac{\gamma_{12}^2}{2} \frac{1 + \sqrt{1 - (\Delta n/2)^2 - \gamma_{12}^2}}{(\Delta n/2)^2 + \gamma_{12}^2}, & \text{if } \gamma_{12}^\infty < \gamma_{12} < \gamma_{12}^0, \\ \Delta n/4, & \text{if } |\gamma_{12}| < \gamma_{12}^\infty. \end{cases} \quad (14)$$

A similar calculation yields the analytical expression for the interaction-energy functional of a dimer having different Coulomb repulsion integrals  $U_1$  and  $U_2$  on each site. Such a generalization is appropriate for applications to models having alternating on-site interactions on bipartite lattices.<sup>40</sup>

Despite their simplicity, Eqs. (13) and (14) reproduce several important exact properties that are common to all systems: (i) The definition of  $W[\gamma]$  is conditioned by the domain of  $v$  representability of the NN bound order  $\gamma_{12}$ , which is given by  $\gamma_{12}^\infty \leq \gamma_{12} \leq \gamma_{12}^0$ . The lower bound  $\gamma_{12}^\infty$  corresponds to the strongly correlated limit and represents the maximum electron delocalization under the constraint of minimal double occupations. The upper bound  $\gamma_{12}^0$  is the noninteracting limit of  $\gamma_{12}$  yielding the maximum degree of delocalization, irrespective of the value of the double occupations. Notice that both  $\gamma_{12}^\infty$  and  $\gamma_{12}^0$  depend on the band filling  $n$ , on the charge transfer  $\Delta n$ , and on the NN connectivity of the specific lattice under study. For the half-filled dimer ( $n = 1$ ) we have  $\gamma_{12}^\infty = \sqrt{\Delta n(2 - \Delta n)}/2$  and  $\gamma_{12}^0 = \sqrt{1 - (\Delta n/2)^2}$ . (ii) At the noncorrelated limit, the underlying electronic state  $\Psi[\gamma_{12}^0]$  is a single Slater determinant and  $W(\gamma_{12}^0) = W^{\text{HF}} = UN_a[n^2 + (\Delta n/2)^2]/4$ .<sup>39</sup> Moreover,  $\partial W/\partial \gamma_{12}$  diverges for  $\gamma_{12} = \gamma_{12}^0$ . This is a necessary condition in order that an arbitrary small  $U$  yields a nonvanishing change in the ground-state density matrix  $\gamma_{12}^{\text{gs}}$ , as expected from perturbation theory.

(iii) For any fixed charge distribution  $\{\gamma_{ii}\}$ ,  $W$  decreases with decreasing  $\gamma_{12}$ , reaching its lowest possible value  $W^\infty = UN_a[\max(n - \Delta n/2 - 1, 0) + \max(n + \Delta n/2 - 1, 0)]/2$  for  $\gamma_{12} = \gamma_{12}^\infty$ . The monotonic decrease in  $W$  upon reducing  $\gamma_{12}$  means that any drop in the Coulomb energy resulting from correlations is achieved at the expense of kinetic energy or electron delocalization. Notice that in most cases  $\gamma_{12}^\infty > 0$ . Reducing  $\gamma_{12}$  beyond  $\gamma_{12}^\infty$  cannot lead to any further decrease in  $W$  for the given  $\{\gamma_{ii}\}$ . Therefore,  $W$  is constant and equal to  $W^\infty$  in the range of  $|\gamma_{12}| \leq \gamma_{12}^\infty$ . (iv) The strongly correlated  $\gamma_{12}^\infty$  shows a nonmonotonous dependence on charge transfer  $\Delta n$ . On a bipartite lattice  $\gamma_{12}^\infty$  vanishes for  $\Delta n = 2 - 2n$  if  $n \geq 1/2$ . In this case, all sites of one sublattice contain strictly one electron, while the sites of the other sublattice contain  $2n - 1$  electrons ( $\gamma_{22} = 1$  and  $\gamma_{11} = 2n - 1$ ). Since the occupation of one of the sublattices is equal to one, no electronic hopping can occur in the strongly correlated limit. In addition,  $\gamma_{12}^\infty$  also vanishes for extreme charge transfers, where one of the sublattices is completely empty ( $\gamma_{22} = 2n$ ,  $\gamma_{11} = 0$ , and  $\Delta n = 2n$ , for  $n \leq 1$ ) or completely full ( $\gamma_{22} = 2$ ,  $\gamma_{11} = 2n - 2$ , and  $\Delta n = 4 - 2n$ , for  $n \geq 1$ ). In this case the uncorrelated  $\gamma_{12}^0$  also vanishes.

The general validity of these properties relies on the universality and transferability of the interaction-energy functional. In order to exemplify the previous general trends we present in Fig. 1 results for  $W_{\text{sc}}$  as a function of  $g_{12}$  for different representative values of  $\Delta n$ . To evaluate the accuracy of the scaled dimer approximation these results are compared with the exact Levy-Lieb functional  $W_{\text{ex}}[\gamma]$ , which was calculated by performing the minimization in Eq. (5) for a finite ring having  $N_a = 10$  sites and different numbers of electrons  $N_e$ . The constraints on  $|\Psi\rangle$  given by Eq. (6) are imposed for  $i = j$  ( $\gamma_{11} + \gamma_{22} = 2n$  and  $\gamma_{22} - \gamma_{11} = \Delta n$ ) and for NN  $ij$  along a periodic ring ( $\gamma_{ij} = \gamma_{12}$ ) by using the method of Lagrange multipliers. In this way the constrained minimization amounts to computing the ground state of an effective Hubbard model, which has been done numerically by means of the Lanczos method.<sup>23,31</sup> The calculations demonstrate the above discussed trends (i)–(iv). In addition, one observes that the proposed approximation  $W_{\text{sc}}$  follows quite closely the exact functional  $W_{\text{ex}}$  all along the crossover from weak to strong correlations (see Fig. 1). This is quite remarkable taking into account the strong dependence of the boundary values  $W^0$ ,  $W^\infty$ ,  $\gamma_{12}^0$ , and  $\gamma_{12}^\infty$  on band filling  $n$  and charge transfer  $\Delta n$ . The quantitative discrepancies are in general small [i.e.,  $|W_{\text{sc}} - W_{\text{ex}}|/(W^0 - W^\infty) \simeq 0.008\text{--}0.06$ ] except for  $N_e = 6$  and  $\Delta n = 1$ , where  $|W_{\text{sc}} - W_{\text{ex}}|/(W^0 - W^\infty) \simeq 0.1$ . Moreover, the largest deviations between  $W_{\text{sc}}$  and  $W_{\text{ex}}$  occur for rather large values of  $\gamma_{12}$  ( $g_{12} \simeq 0.8\text{--}0.9$ ) which concern mainly the weakly correlated regime where the kinetic energy dominates. Consequently, a good general performance of the method can be expected. Although the dependence of  $W$  on the degree of delocalization  $g_{12}$  is similar for different  $\Delta n$ , one observes significant differences between Figs. 1(a)–1(d), which reflect the changes in the nature of the electronic correlations as we move from purely metallic to strongly ioniclike bonds. These are well reproduced by the scaling ansatz  $W_{\text{sc}}$ . In the following section several applications of LDFT are presented by using  $W_{\text{sc}}$  as an approximation to the interaction-energy functional.

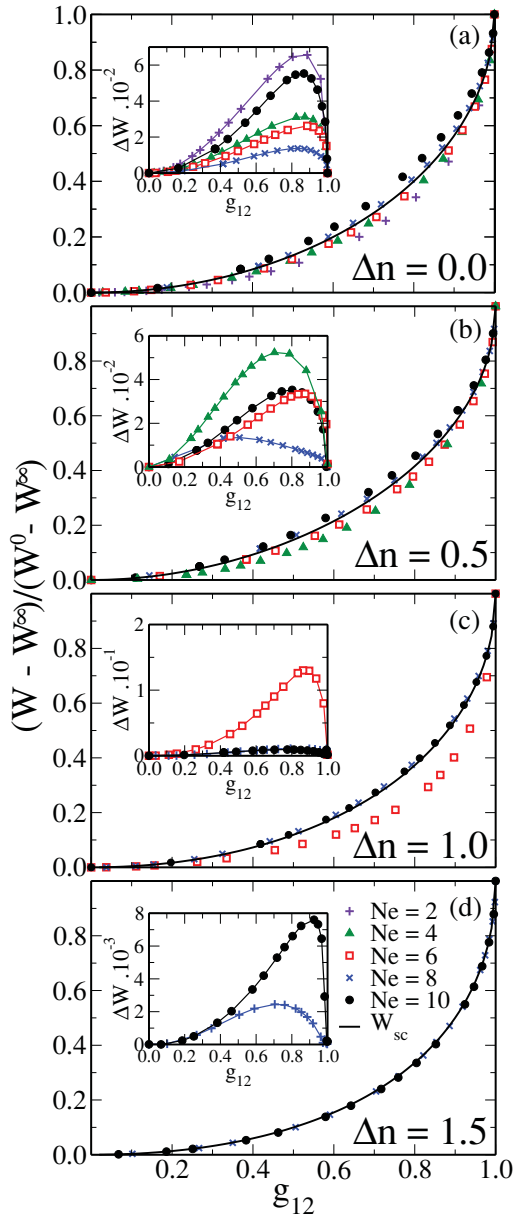


FIG. 1. (Color online) Comparison between the scaled dimer functional  $W_{sc}[\gamma]$  as a function of the degree of electron delocalization  $g_{12} = (\gamma_{12} - \gamma_{12}^{\infty})/(\gamma_{12}^0 - \gamma_{12}^{\infty})$  [solid curves, Eq. (13)] and the exact functional  $W_{ex}$  derived from Lanczos diagonalizations (symbols). Results are shown for a 1D bipartite ring having  $N_a = 10$  sites, different band fillings  $n = N_e/N_a$ , and representative charge transfers  $\Delta n = \gamma_{22} - \gamma_{11}$ . The inset figures display the corresponding relative errors  $\Delta W = (W_{sc} - W_{ex})/(W^0 - W^{\infty})$ .

#### IV. RESULTS AND DISCUSSION

For the applications of the theory we consider the inhomogeneous Hubbard model on bipartite 1D and 2D lattices consisting of a sublattice  $\mathcal{S}_1$ , where the energy levels  $\varepsilon_i = \varepsilon_1 = \varepsilon/2$ , and a sublattice  $\mathcal{S}_2$ , where  $\varepsilon_i = \varepsilon_2 = -\varepsilon/2$  [see Eq. (1)]. Besides the band-filling  $n = N_e/N_a$ , the system is characterized by two dimensionless parameters: the bipartite potential  $\varepsilon/t$ , which controls the degree of charge transfer  $\Delta n = \gamma_{22} - \gamma_{11}$  between the sublattices, and the Coulomb

repulsion strength  $U/t$ , which measures the importance of correlations. The ground-state properties of the model are the result of a subtle interplay between the kinetic energy associated with electronic hopping and delocalization, which is proportional to  $t\gamma_{12}$ , the charge-transfer energy  $\Delta E_{CT} = -\varepsilon\Delta n/2$ , and the Coulomb-repulsion energy  $W$ . The physical behavior is analyzed from the homogeneous to the strongly ionic regimes, as well as from weak to strong correlations, by computing the ground-state energy  $E_{gs}$ , the NN bond order  $\gamma_{12}$ , the charge transfer  $\Delta n$ , the average number of double occupations per site  $W/UN_a$ , and the charge gap  $\Delta E_c$ . The accuracy of the scaled dimer approximation is quantified by comparing systematically the LDFT results with exact Lanczos diagonalizations<sup>32</sup> on finite 1D rings or 2D squares with periodic boundary conditions. These systems also provide an interesting opportunity to assess the ability of LDFT to deal with discrete single-particle spectra and with possible degeneracies at the Fermi energy, which often lead to nontrivial charge transfers as a function of the model parameters.

Figure 2 shows the ground-state properties of a 1D ring having  $N_a = 14$  sites and half-band filling  $n = 1$  as a function of the Coulomb repulsion strength for different values of the energy-level shift  $\varepsilon/t$ . The results are given as a function of  $U/(U + 4t)$  in order to cover the complete interaction range, from weak correlations  $U/t \ll 1$  all over to the strongly correlated limit ( $U/t \gg 1$ ). Notice that  $w_{1D} = 4t$  represents the single-particle bandwidth in 1D. Moreover,  $U/t \simeq 4$  corresponds approximately to the crossover from weak to strong coupling also in higher dimensions. First of all, for the homogeneous case ( $\varepsilon/t = 0$  and  $\Delta n = 0$ ) one observes the well-known monotonous increase of  $E_{gs}$  with increasing  $U/t$ , reaching  $E_{gs} = 0$  for  $U/t \rightarrow \infty$ , where both electronic hopping and double occupations vanish. At the same time  $\gamma_{12}$  and  $W$  decrease monotonously with  $U/t$  [see Figs. 2(b) and 2(d)]. A number of new features appear when the bipartite level shift  $\varepsilon$  is finite. In this case, as we go from weak to strong correlations, the system undergoes a qualitative change from a delocalized charge-density-wave (CDW) state ( $\Delta n \simeq 0.9$ – $1.6$  and  $\gamma_{12} \simeq 0.3$ – $0.6$ ) to a nearly localized state having a homogeneous charge distribution ( $\Delta n < 0.01$  and  $\gamma_{12} < 0.1$ ). Starting from the weakly correlated CDW state and increasing  $U/t$ , one observes a decrease in  $\Delta n$ , since inhomogeneous charge distributions necessarily imply larger average double occupations [see Figs. 2(c) and 2(d)]. Nevertheless, a nearly homogeneous charge distribution is only reached for  $U \gg \varepsilon$ . An interesting effect, which becomes more distinctive as  $\varepsilon/t$  increases, is the nonmonotonous dependence of the kinetic energy and bond order  $\gamma_{12}$  as a function of  $U/t$ . Notice that the maximum in  $\gamma_{12}$  does not correspond to the noninteracting limit but to a finite value of  $U/t$  [see Fig. 2(b)]. In fact, for  $U \simeq \varepsilon$  the Coulomb repulsion on the doubly occupied sites on sublattice  $\mathcal{S}_2$  compensates the energy difference between the two sublattices ( $\varepsilon_1 = \varepsilon/2 = -\varepsilon_2 > 0$ ). This allows a nearly freelike motion of the  $\gamma_{11}$  electrons occupying sublattice  $\mathcal{S}_1$ , together with the extra  $\gamma_{22} - 1$  electrons on sublattice  $\mathcal{S}_2$  ( $\gamma_{11} < \gamma_{22}$  for  $\varepsilon > 0$ ). Consequently, the delocalization of the electrons is enhanced for  $U \simeq \varepsilon$ , yielding a maximum in  $\gamma_{12}$ . The effect is more pronounced for  $\varepsilon/t \gg 1$ , since this implies a stronger CDW at  $U = 0$  and a larger crossover value of  $U = \varepsilon$ . Moreover, it is interesting to observe that

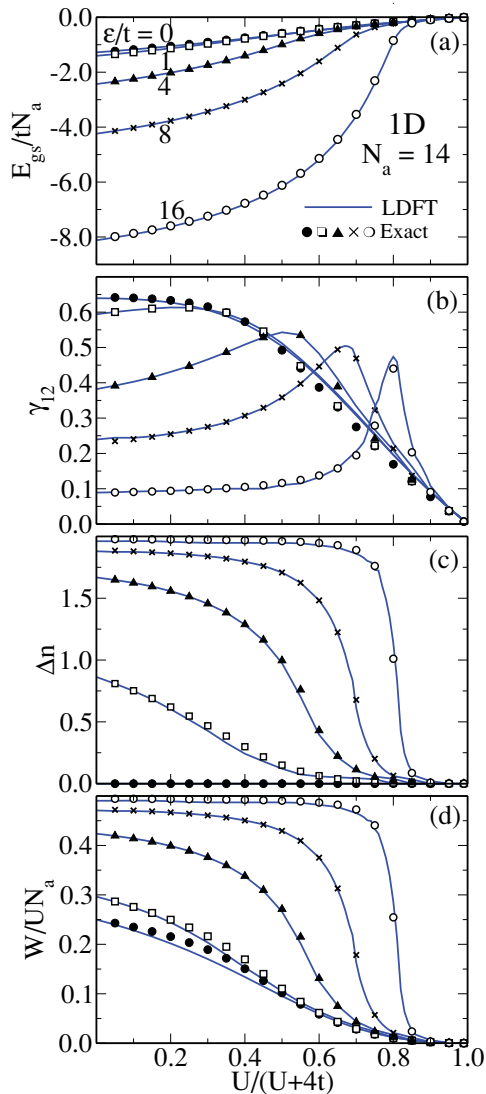


FIG. 2. (Color online) Ground-state properties of bipartite Hubbard rings having  $N_a = 14$  sites and half-band filling  $n = 1$  as a function of the Coulomb repulsion strength  $U/t$ . Different values of the energy-level shift  $\varepsilon$  between the sublattices are considered as indicated in panel (a). Results are given for (a) ground-state energy  $E_{\text{gs}}$ , (b) NN bond order  $\gamma_{12}$ , (c) charge transfer  $\Delta n = \gamma_{22} - \gamma_{11}$ , and (d) average number of double occupations per site  $W/UN_a$ . The solid curves refer to LDFT using the scaling approximation  $W_{\text{sc}}$  [see Eq. (13)] while the symbols are the results of exact Lanczos diagonalizations.

for large  $\varepsilon$  the maximum in  $\gamma_{12}$  corresponds to  $\Delta n = 1$  [compare Figs. 2(b) and 2(c)]. Indeed, for  $U/t \simeq \varepsilon/t \gg 1$  (in practice  $U/t \simeq \varepsilon/t \geq 4$ ) one electron is essentially locked in the sublattice  $\mathcal{S}_2$ , and the remainder electron in the unit cell is evenly distributed among the two sublattices. For  $n = 1$  this implies  $\gamma_{11} \simeq 1/2$  and  $\gamma_{22} \simeq 3/2$ , or equivalently,  $\Delta n = 1$ .

The local magnetic moments  $S_i^2 = \frac{3}{4} \langle (\hat{n}_{i\uparrow} - \hat{n}_{i\downarrow})^2 \rangle = \frac{3}{4} (\gamma_{ii} - 2\langle \hat{n}_{i\uparrow} \hat{n}_{i\downarrow} \rangle)$  at the different sites  $i$  provide an alternative perspective of the electronic correlation and localization occurring as  $U/t$  increases. If one focuses on  $S = 0$  states,  $S_i^2$  can be directly interpreted as the variance of the local magnetic moment. In the uncorrelated limit,  $\hat{n}_{i\uparrow} \hat{n}_{i\downarrow} = \gamma_{ii}^2/4$

and therefore  $S_i^2$  depends only on the density distribution  $\gamma_{ii}$ . For example, for  $n = 1$  one observes that  $S_i^2$  decreases with increasing  $\varepsilon/t$ , namely, from  $S_i^2 = 3/8$  for  $\varepsilon/t = 0$  to  $S_i^2 = 0$  for  $\varepsilon/t = \infty$ . In the latter case all electrons are paired on one sublattice ( $U = 0$  and  $n = 1$ ). If now the Coulomb repulsion is raised, one finds a reduction of charge fluctuations and thus an enhancement of  $S_i^2$ . Finally, for  $U/t \gg 1$  and  $U \gg \varepsilon$  the largest possible  $S_i^2 = 3/4$  is reached, irrespective of the value of  $\varepsilon/t$ . At this point all sites are singly occupied and the variance of  $S_i^2$  is maximal ( $S = 0$ ).

Concerning the comparison between LDFT and exact results one observes that all the considered ground-state properties are very well reproduced by the scaled dimer ansatz. This holds for all values of the energy-level shift between the sublattices, not only close to the weak and strongly correlated limits but also in the intermediate interaction region. Moreover, the fact that  $\gamma_{12}$ ,  $\Delta n$ , and  $W$  are all obtained with a high level of precision shows that the results for  $E_{\text{gs}}$  are not the consequence of a strong compensation of errors. It is also interesting to note that the accuracy actually improves as the charge distribution becomes more inhomogeneous, i.e., as  $\varepsilon/t$  and the CDW become stronger. In other words, the homogeneous case, which was investigated in some detail in Refs. 23 and 24, is the most difficult one. This seems reasonable, since large values of  $\varepsilon$  enhance the importance of single-particle contributions to the energy and somehow tend to decouple the 1D chain in dimers, within which correlations are taken into account exactly. A similar improvement of the accuracy of the scaled dimer functional has already been observed in dimerized chains with homogeneous charge density.<sup>25</sup> One concludes that LDFT, combined with Eqs. (13) and (14) for  $W[\gamma]$ , provides a very good description of electron correlations and of the resulting interplay between kinetic, charge-transfer, and Coulomb energies in 1D lattices.

In Fig. 3 the band-filling dependence of  $E_{\text{gs}}$  is shown for a 1D ring having  $N_a = 14$  sites and representative values of the Coulomb repulsion  $U/t$  and of the energy-level shift  $\varepsilon/t$ . For low electron densities, up to quarter-band filling  $n = 1/2$ , one observes that  $E_{\text{gs}}$  decreases for all  $U/t$  as the band is filled up. Notice in particular the weak dependence of  $E_{\text{gs}}$  on the Coulomb repulsion strength, even for  $U/t \gg 1$ . This implies that for low carrier densities charge fluctuations are very efficiently suppressed by correlations. Consequently, the kinetic and crystal-field energies dominate over the Coulomb energy ( $n \leq 1/2$ ). This is quite remarkable, since ignoring correlations would have led to a quadratic increase in the Coulomb energy ( $E_{\text{HF}} \propto Un^2$ ). Comparing different crystal fields  $\varepsilon/t$ , one notes that the role of electron interactions is most important in the homogeneous case, where our results coincide with previous calculations.<sup>24</sup> As  $\varepsilon/t$  increases the electrons tend to be localized on one sublattice in order to take advantage of the crystal field, thereby reducing the importance of both kinetic and Coulomb contributions. Consequently,  $E_{\text{gs}}$  is nearly independent of  $U/t$  ( $\varepsilon/t \geq 4$  and  $n \leq 1/2$ ). Beyond quarter-band filling the  $n$  dependence of  $E_{\text{gs}}$  changes qualitatively, since double occupations become unavoidable, not only for delocalized electronic states but also for ionic states with significant charge transfer to the most stable sublattice. In this case ( $n \geq 1/2$ )  $E_{\text{gs}}$  continues to decrease with increasing  $n$  only if the Coulomb interactions are weak

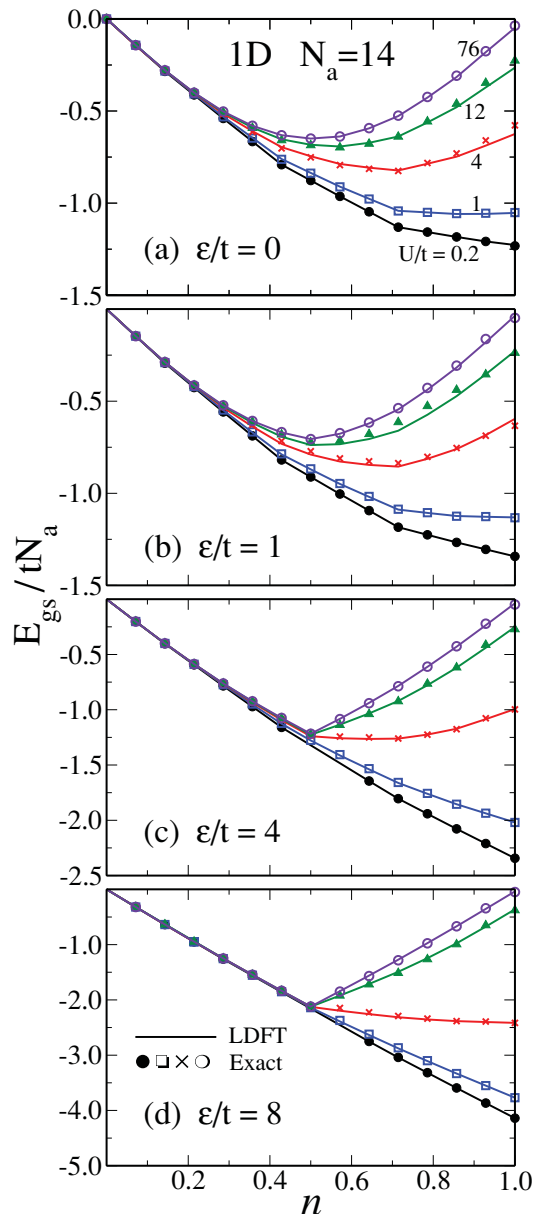


FIG. 3. (Color online) Band-filling dependence of the ground-state energy of 1D Hubbard rings having  $N_a = 14$  sites and different bipartite potentials  $\varepsilon$ . The solid curves refer to LDFT with the scaled dimer functional  $W_{sc}$ , and the symbols refer to exact numerical results. Representative values of the Coulomb repulsion strength  $U/t$  are considered as indicated in panel (a).

( $U/t < 4$ ). Otherwise, for  $U/t > 4$ ,  $E_{gs}$  goes first over a minimum at  $n = 1/2$ , where the decrease in kinetic and crystal-field energies is approximately canceled by the increase in Coulomb energy. Then, it increases with  $n$  as we move to even higher densities ( $n > 1/2$ ). These trends are qualitatively similar for all values of the bipartite potential. However, the crossover from low- to high-density behavior becomes more abrupt as  $\varepsilon/t$  increases [compare Figs. 2(a)–2(d)]. As in Fig. 2 the agreement between the LDFT results (solid curves) and the Lanczos diagonalizations (symbols) is most satisfying for all values of  $n$ ,  $U$ , and  $\varepsilon$ . The scaling approximation reproduces all the previous trends very accurately. Moreover, as already

mentioned in the context of Fig. 2, the quality of the results for  $E_{gs}$  is not the consequence of a compensation of errors on different contributions (i.e.,  $E_{CD}$ ,  $E_K$ , and  $W$ ). This is probably the reason behind the favorable outcome for all band fillings and interaction parameters.

The charge-excitation gap

$$\Delta E_c = E(N_e + 1) + E(N_e - 1) - 2E(N_e) \quad (15)$$

is a property of considerable interest in strongly correlated systems, which measures the insulating or metallic character of the electronic spectrum as a function of  $\varepsilon/t$ ,  $U/t$ , and  $n$ . It can be directly related to the discontinuities in the derivatives of the single-particle and correlation energies per site with respect to the electron density  $n$ . Therefore, the calculation of  $\Delta E_c$  constitutes a more serious challenge than the calculation of  $E_{gs}$ , particularly in the framework of a density-functional approach. In Fig. 4 results are given for  $\Delta E_c$  as a function of band filling  $n < 1$ , which correspond to 1D Hubbard rings having  $N_a = 14$  sites and different  $\varepsilon/t$  and  $U/t$ . The half-filled-band case deserves special attention and is considered in Fig. 5.

Finite bipartite rings have a discrete single-particle energy spectrum, which is conditioned by the two important inversion and electron-hole symmetries. The former requires  $\varepsilon_\alpha(k) = \varepsilon_\alpha(-k)$ , where  $\alpha = 1, 2$  refers to the two bands of the unit cell, and the latter implies that for each eigenenergy  $\varepsilon_\alpha(k)$  the inverse  $-\varepsilon_\alpha(k)$  is also an eigenvalue. In the following we restrict ourselves to  $N_a$  even, as imposed by the periodic boundary conditions. In the homogeneous case ( $\varepsilon = 0$ ) we have one atom per unit cell and  $-\pi/a \leq k \leq \pi/a$ . The single-particle energies are given by  $\varepsilon_k = -2t \cos(ka)$ , where  $k = 0$ ,  $k = \pm \nu\pi/aN_a$ , with  $\nu = 1, \dots, (N_a - 1)$ , and  $k = \pi/a$ . For  $N_a/2$  even, this yields a doubly degenerate level in the middle of the band corresponding to  $k = \pm\pi/2a$ , while for  $N_a/2$  odd  $k = \pm\pi/2a$  is not allowed and there is a gap in the middle of the band between two doubly degenerate states ( $k = \pm 4\pi/7a$  and  $k = \pm 5\pi/7a$  for  $N_a = 14$ ). For  $N_a/2$  even, the alternating bipartite potential ( $\varepsilon \neq 0$ ) couples the states having  $k = \pm\pi/2a$  and opens a gap  $\varepsilon$  at half-band filling ( $n = 1$ ), while for  $N_a/2$  odd, one observes simply an enhancement of the existing gap between doubly degenerate states. The results for  $\Delta E_c$  in the noninteracting limit ( $U/t \ll 1$ ) can be interpreted in terms of the single-particle spectrum. In particular for  $N_a = 14$  one finds that for  $U = 0$  the charge gap  $\Delta E_c = 0$  for  $N_e = 3-5, 7-9$ , and  $11-13$  due to the presence of double degenerate states. Any small Coulomb interaction  $U \neq 0$  removes the double degeneracy yielding a finite  $\Delta E_c$  for  $N_e = 4, 8$ , and  $10$ . This explains the even-odd alternations as a function of  $N_e$  for small  $U/t$  [see Figs. 4(a) and 4(b)].

For strong interactions ( $U/t > 4$ ) the single-particle picture breaks down and simple detailed interpretations seem difficult. One may however observe that for low carrier density ( $n < 1/2$ ) the gap tends to decrease as  $\varepsilon/t$  increases, even for large  $U/t$ , since the two sublattices progressively decouple from each other. In contrast, an increasingly important gap develops for large  $U/t$  at  $n = 1/2$ , which tends to  $\Delta E_c = \varepsilon$  for  $U/t \rightarrow +\infty$ . This contrasts with the corresponding gap in the weakly correlated limit, which vanishes for  $N_a/2$  odd and is finite (of the order of  $t/N_a$ ) for  $N_a/2$  even. The origin of the finite charge

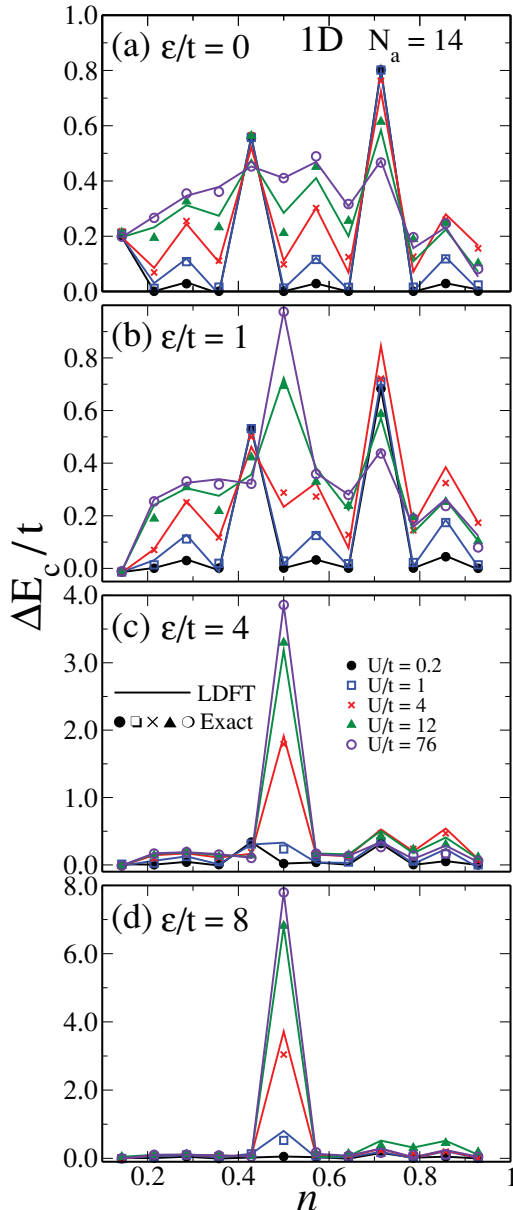


FIG. 4. (Color online) Charge gap  $\Delta E_c = E(N_e + 1) + E(N_e - 1) - 2E(N_e)$  as a function of band filling  $n$  in 1D Hubbard rings having  $N_a = 14$  sites and different bipartite potentials  $\varepsilon$ . The solid lines connecting discrete points refer to LDFT with the scaled dimer functional and the symbols to exact Lanczos diagonalization. Representative values of the Coulomb repulsion strength  $U/t$  are considered as indicated in panel (c). Results for  $n = 1$  are given in Fig. 5.

gap for large  $U/t$  is the energy difference between adding an electron in the sublattice  $S_1$  (having  $\varepsilon_1 = \varepsilon/2$ ) and removing an electron in the sublattice  $S_2$  (having  $\varepsilon_2 = -\varepsilon/2$ ). In fact, for  $U/t \gg 1$  the kinetic energy is very weak,  $E_{CD}$  dominates over  $E_K$ , and therefore the sublattice  $S_1$  is essentially empty in the strongly correlated ground state ( $n \leq 1/2$ ). Notice that a finite  $\Delta E_c \simeq \varepsilon$  for  $n = 1/2$  and large  $U/t$  is also found in the thermodynamic limit, as well as for finite  $N_a$  with  $N_a/2$  even.

As for any excitation, obtaining accurate results for  $\Delta E_c$  within a density-functional approach is more delicate than for

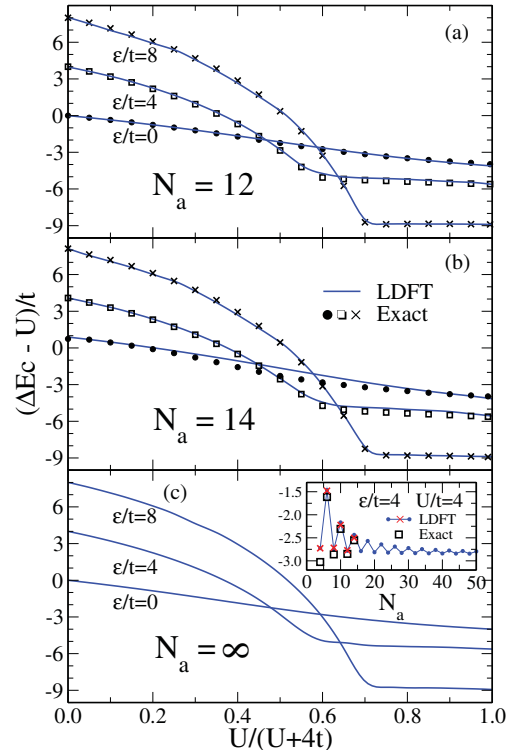


FIG. 5. (Color online) Charge gap  $\Delta E_c = E(N_e + 1) + E(N_e - 1) - 2E(N_e)$  as a function of the Coulomb repulsion strength  $U/t$  in 1D Hubbard rings having a band filling  $n = 1$ , representative values of the bipartite potential  $\varepsilon$ , and (a)  $N_a = 12$ , (b)  $N_a = 14$ , and (c)  $N_a = \infty$  sites. The curves refer to LDFT with the scaled dimer functional  $W_{sc}$  and the symbols to exact diagonalizations. In the inset figure the ring-length dependence of  $(\Delta E_c - U)/t$  is shown for  $\varepsilon/t = 4$  and  $U/t = 4$ .

the ground-state properties. Nevertheless, it seems fair to say that LDFT with the present approximation to  $W$  performs quite well quantitatively, except for intermediate values of  $\varepsilon/t$  and  $U/t$  [see, for example,  $\varepsilon/t = 1$  and  $U/t = 12$  in Fig. 4(b)]. In particular the removal of degeneracies due to the interactions and the resulting even-odd oscillations, the crossover from weak to strong correlations, and the development of a finite gap  $\Delta E_c \simeq \varepsilon$  at quarter-band filling for  $U/t \gg 1$  are very well reproduced.

The charge gap at half-band filling has the specificity of involving an extra double occupation for  $N_e = N_a + 1$ , which is unavoidable even in a strongly correlated state, in contrast to any smaller band filling  $N_e \leq N_a$ . This implies that a contribution of the order of  $U/t$  to  $\Delta E_c$  must be taken for granted. It is therefore more meaningful to consider  $(\Delta E_c - U)/t$  as reported in Fig. 5, which represents the nontrivial kinetic and correlation contributions. In the homogeneous case without interactions ( $\varepsilon = 0$  and  $U = 0$ ) the gap vanishes for  $N_a/2$  even, while it remains of the order of  $t/N_a$  for  $N_a/2$  odd.  $\Delta E_c - U$  decreases monotonously as  $U/t$  increases, reaching a common limit  $\Delta E_c = U - 2w_b$  for all  $N_a$ , where  $w_b$  represents the kinetic energy gained through the delocalization of the extra electron or hole. In the homogeneous case  $w_b = 2t$  coincides with the single-particle band width, since the ground state for  $N_e = N_a \pm 1$  is the fully polarized ferromagnetic Nagaoka

state.<sup>10</sup> The structureless shape of  $\Delta E_c$  as a function of  $U/t$  hides a profound change in the nature of the underlying charge excitation along the crossover from weak to strong interactions, namely, from a single-particle electron-hole excitation to a strongly correlated low-spin to high-spin excitation.<sup>8-10</sup> The simplicity  $\Delta E_c$  versus  $U/t$  should not understate the merit of the LDFT results in comparison to exact diagonalizations ( $N_a = 12$  and  $14$ ).

For nonvanishing bipartite potential and  $U = 0$  the charge gap is positive, equal to  $\varepsilon$  for  $N_a/2$  even, and slightly larger than  $\varepsilon$  for  $N_a/2$  odd (for example, for  $N_a = 14$ ,  $\Delta E_c/t = 1.32$ ,  $4.08$ , and  $8.08$  for  $\varepsilon/t = 1$ ,  $4$ , and  $8$ , respectively). The underlying excitation involves the promotion of an electron across the single-particle gap opened by the bipartite potential. This corresponds to delocalized electron-hole excitations between CDW states, which are more or less strong depending on the value of  $\varepsilon/t$ . As  $U/t$  increases  $\Delta E_c - U$  decreases and eventually changes sign, since the Coulomb repulsion brings the energy of the states with doubly occupied configurations on sublattice  $S_2$  closer to the energy of singly occupied configurations on sublattice  $S_1$  ( $\varepsilon_1 = -\varepsilon_2 = \varepsilon/2 > 0$ ). For  $U > \varepsilon$  the system undergoes a transition to a homogeneous state, after which the gap becomes essentially linear in  $U$ . In the strongly correlated limit  $\Delta E_c = U - 2w_b$  for all  $N_a$ , where, as in the homogeneous case,  $w_b$  represents the energy gained through the addition of the extra electron or hole. These are the same due to the electron-hole symmetry of the bipartite lattice. In the homogeneous case, the extra electron occupies the  $k = 0$  state of the minority-spin band, while the majority band is full (Nagaoka state).<sup>10</sup> Therefore,  $w_b = 2t$  coincides with the single-particle bandwidth. In the presence of a finite bipartite potential the situation is similar, since an extension of Nagaoka's theorem also holds in the presence of inhomogeneous energy levels  $\varepsilon_i$ .<sup>11</sup> However, notice that the bipartite potential introduces a shift of the energy  $\varepsilon_0$  of the  $k = 0$  single-particle state, which stabilizes the system with  $N_e = N_a \pm 1$  electrons relative to the half-filled case ( $N_e = N_a$ ). For example,  $\varepsilon_0/t = -2.83$  for  $\varepsilon/t = 4$  and  $\varepsilon_0/t = -4.47$  for  $\varepsilon/t = 8$ . Consequently, the strongly correlated limit of  $(\Delta E_c - U)/t$  decreases with increasing  $\varepsilon/t$ .

The comparison between LDFT and exact diagonalizations shows a very good agreement. This confirms the previously observed trend to a slight improvement of accuracy as the strength of the bipartite potential  $\varepsilon/t$  increases. Figure 5 also reports LDFT results for the charge gap in the thermodynamic limit. In this case  $\gamma_{12}^\infty$  is obtained from a Nagaoka-like variational state in which the spin-up orbitals of sublattice  $S_2$  are occupied ( $\gamma_{22} > \gamma_{11}$ ) and the remaining  $\gamma_{11} + \gamma_{22} - 1$  spin-down electrons are delocalized throughout the entire lattice. The trends observed for  $N_a = \infty$  are essentially the same as for  $N_a = 12$  or  $14$ . The dependence of  $\Delta E_c$  on the chain length is given in the inset of Fig. 5(c). The accuracy of the LDFT calculations for different  $N_a$  is quantified by comparison with exact results.

Figure 6 shows the ground-state properties of the 2D Hubbard model on a square cluster having  $N_a = 16$  sites and periodic boundary conditions. The results are given as a function of the Coulomb repulsion strength  $U/t$  for different values of the energy-level shift  $\varepsilon/t$  at half-band filling  $n = 1$ . First of all, one observes a number of qualitative similarities

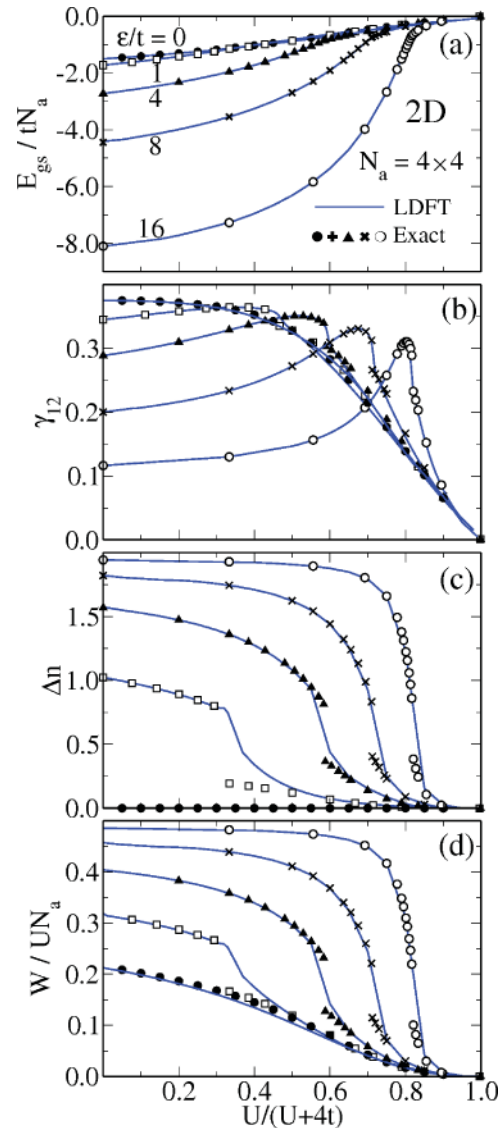


FIG. 6. (Color online) Ground-state properties of the half-filled Hubbard model on a 2D square cluster having  $N_a = 4 \times 4$  sites and periodic boundary conditions ( $n = N_e/N_a = 1$ ). Results are given for (a) ground-state energy  $E_{gs}$ , (b) NN bond order  $\gamma_{12}$ , (c) charge transfer  $\Delta n = \gamma_{22} - \gamma_{11}$ , and (d) interaction energy  $W$ . LDFT (solid curves) and exact diagonalizations (symbols) are compared as a function of the Coulomb repulsion strength  $U/t$  for representative values of the energy level shift  $\varepsilon$  between the sublattices, as indicated in panel (a). The discontinuities in the exact results for  $\gamma_{12}$ ,  $\Delta n$ , and  $W$  are a consequence of the degeneracy of the single-particle spectrum and the finite cluster size.

with the ground-state properties of 1D rings presented in Fig. 2. Among these let us mention the monotonous increase of  $E_{gs}$  with increasing  $U/t$ , the stabilization associated with the bipartite potential  $\varepsilon$ , and the convergence of all  $E_{gs}$  curves to the  $\varepsilon = 0$  case when  $U \gtrsim \varepsilon$  [see Fig. 6(a)]. The convergence of  $E_{gs}$  to the homogeneous limit occurs for  $U/t$  larger than the value at which the NN bond order  $\gamma_{12}$  is maximal, once the charge transfer  $\Delta n = \gamma_{22} - \gamma_{11}$  and the interaction energy  $W$  drop. These features are comparable to the behavior observed in the 1D case and can be understood in similar terms. They

reflect the change from a weakly correlated CDW state to a strongly correlated nearly homogeneous state as the strength of the Coulomb interactions is increased. However, in the present 2D periodic cluster one observes distinctive discontinuities in  $\gamma_{12}$ ,  $\Delta n$ , and  $W$  as a function of  $U/t$ , which are absent in the 1D results for  $N_a = 14$  (compare Figs. 2 and 6). These discontinuities are a finite-size effect resulting from the sixfold degeneracy of the single-particle spectrum at the Fermi energy  $\varepsilon_F$ . They are not specific to the 2D geometry, since similar effects are also found in finite 1D chains with periodic boundary conditions. In the present case, four of the degenerate states at  $\varepsilon_F$  admit a charge transfer of one electron between the sublattices [ $\vec{k} = (\pm\pi/2a, \pm\pi/2a)$ ], while the two others show a homogeneous charge distribution [ $\vec{k} = (\pi/a, 0)$  and  $\vec{k} = (0, \pi/a)$ ]. Two of the former CDW states are stabilized by the bipartite potential, although they involve an average number of double occupations higher than that of the latter. The number of electrons at half-band filling is such that only three of the six degenerate states are occupied for both spin directions ( $U = 0$ ). In the weakly correlated limit and for  $\varepsilon \neq 0$  two of the states with strong charge transfer are occupied. Thus, the ground state corresponds to a CDW state. This configuration remains stable for rather large values of  $U/t$ , until  $U$  becomes larger than  $\varepsilon$ . At this point a sharp transition to a nearly homogeneous state takes place. Shortly before the discontinuities occur  $\gamma_{12}$  goes over a maximum, as the energy to transfer an electron from a doubly occupied site of sublattice  $S_2$  to an empty site on sublattice  $S_1$  vanishes. It is worth noting that such discontinuous jumps only take place for specific band fillings which match the degeneracies of the single-particle spectrum. They are not observed for other band fillings or in the thermodynamic limit. For example, for  $N_e = 10$ , no discontinuities in the ground-state properties are observed, since the Fermi level is not degenerate. The importance of this finite-size effect decreases with increasing system size typically proportional to  $1/N_a$ . In the present case the change in  $\Delta n$  resulting directly from the changes of occupation among the degenerate levels is 0.5, which corresponds to the transfer of two electrons per spin in an  $N_a = 16$  cluster.

Comparison with exact diagonalizations shows that LDFT with the scaled dimer approximation yields quantitatively good results both for  $U$  significantly smaller and larger than  $\varepsilon$ . However, the approximation fails to reproduce the sharp transition. Instead, a continuous crossover is predicted, which becomes sharper and thus more accurate as  $\varepsilon/t$  increases (see Fig. 6). The shortcomings of the scaling approximation can be traced back to the particular form of the pure-state  $v$ -representability domain of the density matrix in the square  $4 \times 4$  cluster, which is composed of two disjoint regions as a function of  $\gamma_{11}$  and  $\gamma_{12}$  for  $\gamma_{11} + \gamma_{22} = 2$ . In other words, the pure-state representability domain is neither convex nor simply connected at half-band filling. It is therefore not surprising that the scaling approximation yields a continuous crossover, since the scaling hypothesis implicitly assumes a convex or at least path-connected representability domain. Nevertheless, aside from this restriction, the overall predictions of LDFT always remain correct. Moreover, in the absence of degeneracies at  $\varepsilon_F$  (e.g., for  $N_e = 12$  and  $N_a = 16$  in 2D) LDFT recovers its usual performance for all model parameters. A more detailed

discussion of the effects of degeneracies on the representability of the density matrix can be found in Ref. 31.

Finally, it is worth noting that the LDFT results for  $E_{gs}$  are invariably very accurate, even close to the transition and despite the discontinuities observed in other exact calculated properties. This is in fact the result of a compensation of errors between the charge-density energy  $E_{CD} = -\varepsilon\Delta n/2$  and the interaction energy  $W$ . Indeed, in the transition region the scaling ansatz overestimates both  $\Delta n$  and  $W$ . In contrast, the bond order and thus the kinetic energy are obtained quite precisely [see Figs. 6(b)–6(d)].

## V. SUMMARY AND OUTLOOK

A density-matrix functional approach to lattice-fermion models has been applied to the inhomogeneous Hubbard Hamiltonian on bipartite 1D and 2D lattices. As in the continuum<sup>1</sup> the kernel of the theory is interaction energy  $W$ , regarded here as a functional of the density matrix  $\gamma_{ij}$  with respect to the lattice sites. Based on previous investigations<sup>31</sup> of the scalability and transferability of  $W[\gamma]$ , and on exact analytical results for the Hubbard dimer, we propose a simple approximation to  $W$ , which takes advantage of its scaling behavior. In this way a unified description of the interplay between correlations and charge redistributions is achieved from weak to strong coupling and for all band fillings. Using this approximation, several important ground-state properties as well as the charge-excitation gap of 1D and 2D lattices have been determined successfully as a function of the Coulomb repulsion strength and of the external bipartite potential.

The accuracy of the results confirm the pertinence of the scaling approximation and the transferability of the interaction-energy functional. Among the reasons for the success of the present scaled dimer approximation one should first of all mention the universality of the correlation-energy functional as stated by Hohenberg-Kohn's or Levy-Lieb's formulations. Moreover, the present approach has the asset of incorporating exact information on  $W[\gamma]$  at the two most important limits of weak and strong correlations. These fundamental boundary conditions—somehow analogous to the sum rules of the local-density approximation in the continuum—provide a useful guide for the development of the theory and are a further reason for the good performance of the method.

In order to go beyond the present study it would be worthwhile to investigate the role played by the on-site form of the Hubbard-Anderson interaction in more detail. For example, it is interesting to generalize the interaction-energy functional to the case of site-dependent Coulomb repulsions, since this would allow a more realistic description of inhomogeneous systems like transition-metal oxides. Such an extension is indeed possible by using a suitably scaled dimer approximation with different on-site repulsions.<sup>40</sup> Moreover, the locality of the dominant interactions is a characteristic of strongly correlated phenomena, which could be exploited more systematically in the future. In this way it should be possible to improve the flexibility of the explicit approximations to  $W[\gamma]$ , thereby extending the range of applicability of LDFT.

- <sup>1</sup>P. Hohenberg and W. Kohn, *Phys. Rev. B* **136**, 864 (1964).
- <sup>2</sup>W. Kohn and L. J. Sham, *Phys. Rev. A* **140**, 1133 (1965).
- <sup>3</sup>R. G. Parr and W. Yang, *Density-Functional Theory of Atoms and Molecules* (Clarendon, Oxford, 1989).
- <sup>4</sup>R. M. Dreizler and E. K. U. Gross, *Density Functional Theory* (Springer, Berlin, 1990) and references therein.
- <sup>5</sup>R. Pariser and R. G. Parr, *J. Chem. Phys.* **21**, 466 (1953); **21**, 767 (1953); J. A. Pople, *Trans. Faraday Soc.* **49**, 1375 (1953).
- <sup>6</sup>P. W. Anderson, *Phys. Rev.* **124**, 41 (1961).
- <sup>7</sup>J. Hubbard, *Proc. R. Soc. London A* **276**, 238 (1963); **281**, 401 (1964); J. Kanamori, *Prog. Theor. Phys.* **30**, 275 (1963); M. C. Gutzwiller, *Phys. Rev. Lett.* **10**, 159 (1963).
- <sup>8</sup>E. H. Lieb and F. Y. Wu, *Phys. Rev. Lett.* **20**, 1445 (1968); H. Shiba, *Phys. Rev. B* **6**, 930 (1972).
- <sup>9</sup>E. H. Lieb, *Phys. Rev. Lett.* **62**, 1201 (1989).
- <sup>10</sup>Y. Nagaoka, *Solid State Commun.* **3**, 409 (1965).
- <sup>11</sup>H. Tasaki, *Phys. Rev. B* **40**, 9192 (1989).
- <sup>12</sup>M. Kollar, R. Strack, and D. Vollhardt, *Phys. Rev. B* **53**, 9225 (1996); **55**, 11878 (1997).
- <sup>13</sup>J. E. Hirsch, *Phys. Rev. B* **31**, 4403 (1985); **35**, 1851 (1987); N. Furukawa and M. Imada, *J. Phys. Soc. Jpn.* **60**, 3604 (1991); **61**, 3331 (1992).
- <sup>14</sup>S. R. White, *Phys. Rev. Lett.* **69**, 2863 (1992); *Phys. Rev. B* **48**, 10345 (1993).
- <sup>15</sup>E. Dagotto, *Rev. Mod. Phys.* **66**, 763 (1994); A. Georges, G. Kotliar, W. Krauth, and M. J. Rozenberg, *ibid.* **68**, 13 (1996); M. Imada, A. Fujimori, and Y. Tokura, *ibid.* **70**, 1039 (1998).
- <sup>16</sup>D. C. Langreth and M. J. Mehl, *Phys. Rev. B* **28**, 1809 (1983); A. D. Becke, *Phys. Rev. A* **38**, 3098 (1988); J. P. Perdew, K. Burke, and M. Ernzerhof, *Phys. Rev. Lett.* **77**, 3865 (1996) and references therein.
- <sup>17</sup>See, for instance, P. Fulde, *Electron Correlations in Molecules and Solids* (Springer, Berlin, 1991); N. H. March, *Electron Correlation in Molecules and Condensed Phases* (Plenum, New York, 1996); G. D. Mahan, *Many-Particle Physics* (Kluwer, New York, 2000).
- <sup>18</sup>O. Gunnarsson and K. Schönhammer, *Phys. Rev. Lett.* **56**, 1968 (1986); A. Svane and O. Gunnarsson, *Phys. Rev. B* **37**, 9919 (1988); K. Schönhammer, O. Gunnarsson, and R. M. Noack, *ibid.* **52**, 2504 (1995).
- <sup>19</sup>A. Schindlmayr and R. W. Godby, *Phys. Rev. B* **51**, 10427 (1995).
- <sup>20</sup>A. E. Carlsson, *Phys. Rev. B* **56**, 12058 (1997); R. G. Hennig and A. E. Carlsson, *ibid.* **63**, 115116 (2001).
- <sup>21</sup>N. A. Lima, M. F. Silva, L. N. Oliveira, and K. Capelle, *Phys. Rev. Lett.* **90**, 146402 (2003).
- <sup>22</sup>C. Verdozzi, *Phys. Rev. Lett.* **101**, 166401 (2008).
- <sup>23</sup>R. López-Sandoval and G. M. Pastor, *Phys. Rev. B* **61**, 1764 (2000).
- <sup>24</sup>R. López-Sandoval and G. M. Pastor, *Phys. Rev. B* **66**, 155118 (2002).
- <sup>25</sup>R. López-Sandoval and G. M. Pastor, *Phys. Rev. B* **67**, 035115 (2003).
- <sup>26</sup>R. López-Sandoval and G. M. Pastor, *Phys. Rev. B* **69**, 085101 (2004).
- <sup>27</sup>M. Levy, *Proc. Natl. Acad. Sci. USA* **76**, 6062 (1979).
- <sup>28</sup>See, for instance, Z.-Q. Yu and L. Yin, *Phys. Rev. B* **81**, 195122 (2010); L. F. Tocchio, F. Becca, and C. Gros, *ibid.* **81**, 205109 (2010).
- <sup>29</sup>M. H. Oliveira, E. P. Raposo, and M. D. Coutinho-Filho, *Phys. Rev. B* **80**, 205119 (2009).
- <sup>30</sup>M. E. Pezzoli and F. Becca, *Phys. Rev. B* **81**, 075106 (2010).
- <sup>31</sup>M. Saubanère and G. M. Pastor, *Phys. Rev. B* **79**, 235101 (2009).
- <sup>32</sup>C. Lanczos, *J. Res. Nat. Bur. Stand.* **45**, 255 (1950); B. N. Parlett, *The Symmetric Eigenvalue Problem* (Prentice Hall, Englewood Cliffs, NJ, 1980).
- <sup>33</sup>The present model can be generalized in order to provide a more realistic description of specific materials, for example, by including several bands, second  $NN$  hoppings, or interatomic Coulomb repulsions. In the context of inhomogeneous charge-density distributions and transition-metal oxides, it seems particularly interesting to take into account a possible site dependence of the Coulomb integrals  $U_i$ .
- <sup>34</sup>T. L. Gilbert, *Phys. Rev. B* **12**, 2111 (1975). For more recent studies, see, for example, S. Goedecker and C. J. Umrigar, *Phys. Rev. Lett.* **81**, 866 (1998) and references therein.
- <sup>35</sup>Notice that the present representability conditions concern the single-particle density matrix. This approach is different from the investigations of the  $N$  representability of second-order reduced density matrices, which would allow an explicit calculation of  $W$ . See, for instance, Ref. 36.
- <sup>36</sup>A. J. Coleman, *Rep. Math. Phys.* **4**, 113 (1973).
- <sup>37</sup>W. Töws and G. M. Pastor, *Phys. Rev. B* **83**, 235101 (2011).
- <sup>38</sup>Numerical results reported in Ref. 31 show that the dependence of  $W$  on  $\Delta n$  is not very strong in general, always much weaker than the dependence on  $g_{12}$ .
- <sup>39</sup>In case of degeneracies at the Fermi energy of the single-particle spectrum in a finite system,  $W^0$  can be calculated by applying degenerate perturbation theory ( $W^0 < W^{\text{HF}}$ ).
- <sup>40</sup>Further details will be published elsewhere.